Tailoring Spectral and Photochemical Properties of Bioinspired Retinal Mimics by in Silico Engineering

Tailoring Spectral and Photochemical Properties of Bio-inspired Retinal Mimics via *in Silico* Engineering

Mohsen M.T. El-Tahawy[a,b], Irene Conti[a], Matteo Bonfanti[a], Artur Nenov*[a], Marco Garavelli*[a]

Abstract: Controlling the spectral tunability and isomerization activity is currently one of the hot topics in the design of photo-reversible molecular switches for application in optoelectronic devices. The present work demonstrates how to manipulate the absorption of the retinal protonated Schiff base (rPSB) chromophore over the entire visible range by targeted functionalization of the retinal backbone. Moreover, we establish a correlation between the vertical excitation energy and the profile of the potential energy surface of the bright excited state responsible for the photoreactivity of rPSB. We exploited this correlation to rank the functionalized rPSB into different classes with characteristic photoisomerization activity. Eventually, the synergic effects of functionalization and of external electric fields in the few MV/cm range have been applied to achieve a reversable and regioselective control of the photoisomerization propensity of selected rPBS derivatives.

Introduction

Retinal protonated Schiff base (rPSB) is the chromophore which is naturally designed to convert light energy into chemical, mechanical, or electrical energies in the rhodopsin family of proteins. rPSB is positively charged with the charge mainly localized on the N-head in both the ground (GS) and double excited S_2 states (that are therefore termed covalent states), whereas a positive charge transfer (CT) towards the C-tail occurs upon excitation in the lowest bright state S_1. The degree of CT is very sensitive to the immediate environment and a modulation of the absorption wavelength over a wide spectral range of 400-600 nm has been documented inside the protein scaffold[1]. Upon photoexcitation, rPSB performs un ultrafast, efficient (> 70%) and selective isomerization[2], driven by a non-adiabatic decay through a conical intersection (CI) between S_1 and S_0. The absorption wavelength dependence on the environment and the ballistic mechanism motivated the concept of hypsochromic shift → high reaction speed / short excited state (ES) lifetime → high quantum yield(QY) in protein-embedded rPSB[2e, 3]. Recently, based on QM/MM mixed quantum classical dynamics simulations in the three animal visual pigments rhodpsin, squidorhodopsin and melanopsin we challenged the correlation between ES lifetime and QY by demonstrating that a high photoisomerization speed does not necessary assure a highly efficient isomerization. Alternatively, we proposed that the keystone for high QY is the phase-matching between different modes [4]. However, we found a correlation between the blue-shift of the absorption wavelength and the time scale on which the CI region is reached, which opens a playground for engineering multifunctional rPSB based photoresponsive molecules by exploiting the absorption wavelength sensitivity to external stimuli.

Tuning of absorption wavelength and photoreactivity of protein embedded rPSBs are thought to be accomplished by manipulating both the steric and the electrostatic interactions with the environment[5]. These interactions can be artificially mimicked by three different approaches. One way is to reengineer the environment through mutation of close lying amino acid residues in designer proteins[3b, 6], therefore altering the local electric field experienced by the chromophore that in the proteins fluctuates in the range of ±0.005 au as demonstrated by experimental electrostatic potential maps[7]. Using this strategy, Wang et al. were able to tune the absorption spectra of the human cellular all-*trans*-retinal binding protein II over the range 440 - 640 nm[6e]. An alternative approach is based on the application of an external electric field (EF). In a recent systematic study[8] we demonstrated how a homogeneous EF parallel to the conjugated chain tunes the absorption wavelength of the rPSB chromophore throughout the entire visible range (400-800nm) and steers the isomerization, potentially converting the rPSB chromophore from a nonfluorescent ultrafast photoisomerizing device into a fluorescent dye. The drawback of this approach lies in the need to apply EF in the range of tens of MV/cm, which parallels the local protein fields, but is definitely not viable for daily life applications in standard Information and Communication Technologies devices and is technically reachable only in proof−of−concept laboratory realizations[9]. The third approach depends on the introduction of functional groups in the chromophore itself. These groups could be seen as generators of non-uniform local strong EF and their introduction in the conjugated system is an integral strategy to improve the flexibility of the artificial rPSBs not only for the purpose of tuning its absorption cross section over the whole visible range but also to control its photoreactivity[5b, 10]. In this regard, an interesting observation was made by Sovdat et al. [10i], who demonstrated that a suitably placed methyl group red-shifts the rPSB absorption in methanol, while drastically decreasing the ES lifetime from ca. 4 ps to 0.55 ps. Demoulin et al.[11] correlated this decrease in lifetime to the topology of the ES potential energy surface (PES), characterized by a barrierless profile to the crossing seam in case of the methylated form.

[a] Prof. Dr. M. Garavelli, Dr. A. Nenov, Dr. Matteo Bonfanti, Dr. Irene Conti, Dr. M. El-Tahawy
Dipartimento di Chimica industriale “Toso Montanari”, Università di Bologna, Viale del Risorigmento 4, 40136 Bologna, Italy
E-mail: marco.garavelli@unibo.it (M.G.); artur.nenov@unibo.it (A.N.); matteo.bonfanti@unibo.it (M.B.) irene.conti@unibo.it (I.C.)
[b] Dr. M. El-Tahawy,
Chemistry Department, Faculty of Science, Damanhour University, Damanhour 22511, Egypt
E-mail: mohsen.eltahawy@sci.dmu.edu.eg

Supporting information (SI) for this article is given via a link at the end of the document

In the present proof−of−concept study based on SS-CASPT2 calculations (see SI for computational details), we explore this functional group approach by performing a thorough exploration of the photophysics of rPSB derivatives functionalized with electron withdrawing (EWG) and/or donating (EDG) functional groups and show the conceptual equivalence of this chemical approach to the effect of an external EF. We rationalize the role of various types of functional groups in the modulation of the absorption spectrum, PES and CI seam topology and quantify the effects. Exploiting the synergy between external EF and functional groups we demonstrate how to fine-tune and, thus, control speed and selectivity of the rPSB photoisomerization without the necessity to apply external fields in the range of tens of MV/cm.

Results and Discussion

1. Influence of the Functionalization on the Absorption Energies

The parent compound R (**Scheme 1**) displays an absorption which peaks at 2.36 eV (525 nm) associated with the lowest bright HOMO → LUMO transition (labeled S_1) acompained with a partial positive CT from the N-head to C-tail. In a recent study we showed that the absorption can be gradually modulated between ~1.5 eV (800 nm) and ~3.1 eV (400 nm) under the effect of electric fields in the range +0.004 au (+20.5 MV/cm) to -0.005 au (-25.7 MV/cm). Such a modulation can be also achieved by functionalizing the parent compound with chemical groups (**Figure 1**, see **Scheme 1** for the chemical structure of R_1→R_{41}). The shift in absorption energy depends on two factors: the electronic nature of the functional groups and their positions along the polyene chain, i.e. a group may amplify or weaken the CT depending on its electronic nature and position, eventually res ulting in a batho- or hypsochromic shift. Below we classify the functional groups according to the nature and strength of their effect on the electronic structure of the parent compound.

i- Charged groups (-NR_4^+): As expected, introducing a positively charged group is the most intuitive and straightforward way to shift the absorption energy in both directions, which most closely reproduces the effects of a homogeneous external field. A positively charged group like -NR_3^+ at the C-terminus (R_{33}, R_{39} and R_{41}) impedes the charge transfer from N-head to the C-terminus, thus inducing a strong blue-shift of more than 1 eV (R_{41}). Instead, introducing a positively charged group at the N-head (R_{12}) induces a strong red-shift.

ii- Inductive effects (-CF_3): replacing a methyl by a CF_3 group at a position closer to the N-tail (R_{19}) or at a position closer to the C-tail (R_{32}) causes an absorption shift of ca. ±0.3 eV with respect to the R. This behavior is easily understood considering that CF_3 is an EDG with a pronounced negative inductive (***-I***) effect. For instance, CF_3 at C_{13} stabilizes the positive CT from the N-head to C-terminus wherein the N-head accommodates less positive charge as evident from the resonant structures dominating the ground and excited state valence-bond wave functions (**Scheme 2**), the relevant structures were proposed based on CASSCF Mulliken charges analysis where C_{13} and C_{15} in the GS and C_7, C_9 and C_{11} in the ES host most of the positive charge(Table S4) in agreement with previously reported study in our group that only odd-numbered positions of the conjugated chain are expected to host the positive charge[12]. At C_9 the situation is reversed so that a CF_3 group (or an EWG in general) placed there destabilizes and, hence, blue-shifts the CT transition. Generally, a shift of comparable magnitude is also observed for a CH_3/CF_3 exchange in other pairs of compounds (i.e. R_8/R_2, R_{17}/R_5, R_{28}/R_{23} and R_{26}/R_{10}). It is worth mentioning that the pair R_{27}/R_{23} shows a blue-shift of only 0.16 eV, a consequence of the extension of the conjugated system by a benzene ring.

iii- Shielding of the charge: (**-OR** and **-NR_2**)**:** The use of an amino or alkoxy groups close to the C-terminus (e.g. at C_9 in R_{14}, R_{16} and R_{18}) displays negligible effects on the absorption energies (compared against R_{19}), the reason being that the groups tend to decouple from the conjugated backbone by rotating along the C-O/C-N bonds of OR and NR_2, respectively. Instead, when placed close to the N- head (i.e. at C_{14}), they orient their lone pair towards the nearby protonated imine in order to effectively shield its positive charge. Such behavior is observed for R_{36}, R_{37}, R_{38} and R_{40} with a particularly strong CT destabilizing effect of ca. 0.60 eV.

iv- Mesomeric effects (**-O-** and **-NR-**)**:** Introducing the lone-pair containing heteroatoms oxygen and nitrogen within a non-aromatic ring in order to prevent rotation and to align their lone pairs to the conjugated plane results in a blue-shift of 0.25 eV for **-O-** (R_{34}) and 0.40 eV for **-NR-** (R_{35}) when the group is placed in the vicinity of the N-head (C_{14}), whereas placement close to the C-terminus (C_7) leads to a red-shift of ca. 0.35 eV (R_3 and R_4 wrt R_{19}). The observed blue- and red-shifts are attributed to the positive mesomeric (***+M***) effect which overcomes their ***-I*** effect. The effect of the positioning of the groups along the chain on the strength of the interaction (i.e. at C_7 and C_9) may be estimated by comparing the pairs R_3/R_{13} and R_4/R_{15}: the closer the functional group to the C-terminus, the more pronounced the red-shift of the transition.

v- Variation of the length of the conjugated system: In general, increasing the length of the conjugated π-system induces a bathochromic shift, that can reach up to 0.15 eV as demonstrated for pairs R/R_{26}, R_{24}/R_{21} and R_{30}/R_{25} where an additional double bond has been introduced in the chain. An effect of a similar magnitude can be also observed when the ß-ionone ring characterized by a dihedral angle C_5−C_6−C_7−C_8 of about 60°-70° in R is replaced by a simple double bond (R_{29}). This is attributed to the increased conjugation strength in the planar R_{29}, free of steric constraints.

vi- Heteroaromatic rings: generally, replacing the ß-ionone ring with a heterocyclic five- or six-membered ring (R_1, R_2, R_5, R_8, R_{17}, R_{27}) decreases the absorption energy due to increasing number of π-bonds and the acquired planarity of the extended conjugated system. Depending on the heteroring, the effect can vary: 1,4-dirhydropyridine (R_1), pyrrole (R_8), furan (R_{17}) and pyridine (R_{27}) show a 0.7 eV, 0.6 eV, 0.3 eV and 0.1 eV red-shift, respectively. Thereby electron rich nitrogen-containing rings have a more pronounced stabilizing effect compared to oxygen-containing ones. Electron-poor heteroaromatic rings (R_{27} functionalized with a pyridine), as well as benzene show a marginal red-shift of ca. 0.1 eV (pairs R_{23}/R and R_9/R_{19}).

In conclusion, a correlation exists between the observed absorption energy shifts and the strength and position of the functional groups, which can be understood considering the equivalent EF induced by those groups. Furthermore, it appears that the electronic effects of simultaneously introduced groups are additive, qualitatively speaking. Absorption energy shifts within ±0.3 eV can be achieved by introducing single groups with ***I*** or ***M*** effects at either terminus of the conjugated chain. Stronger shifts (i.e. above 0.3 eV) become feasible with three scenarios: (i) through functionalization with charged groups; (ii) a combination of two or more additive effects (push-pull functionalization); (iii) replacing the ß-ionone ring with electron rich heterocyclic rings such as pyridine.

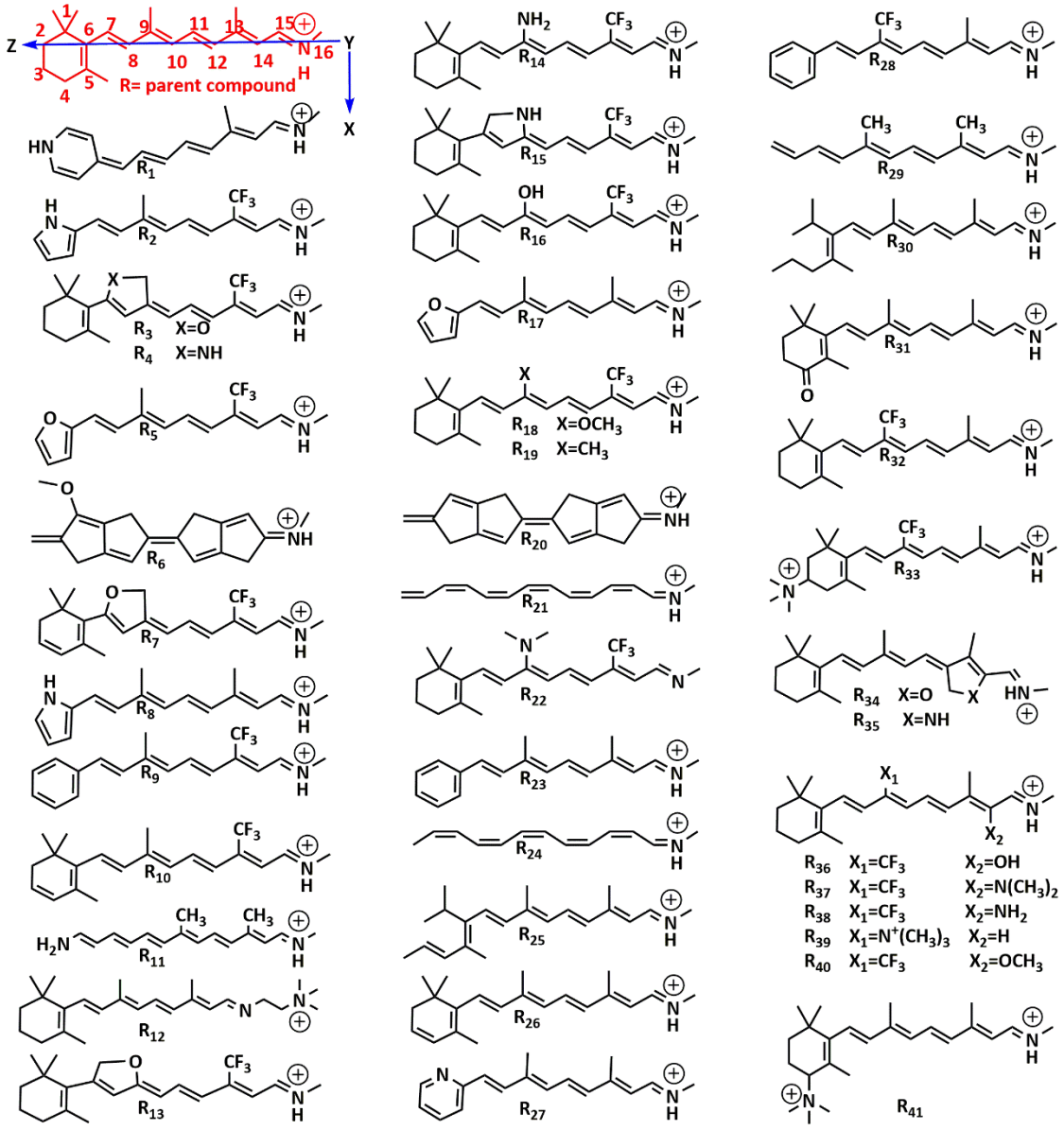

Scheme 1. Functionalized rPSBs R_{1-41}. The numeration of the atoms in the conjugated chain (i.e. C_5 through N_{16}) shown for the parent compound R is adopted for all systems.

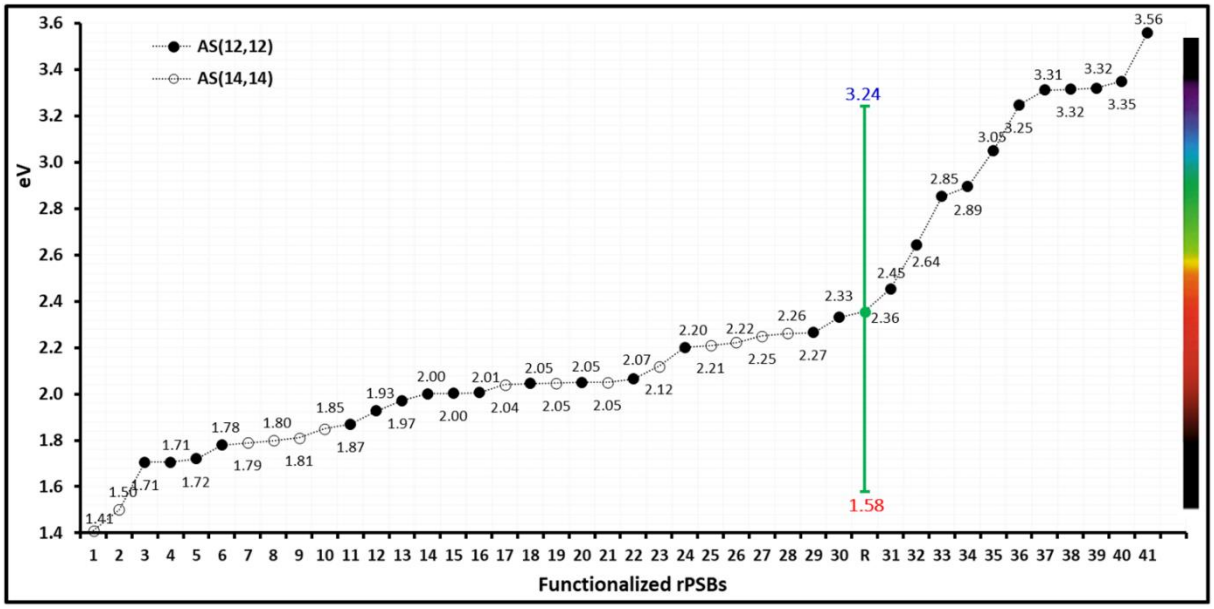

Figure 1. Absorption energies of the functionalized rPSBs R_{1-41} (see **Scheme 1**). The vertical green line indicates the absorption energy shift realized on R by applying a homogeneous external EF in the range of +0.004 to -0.005 au[7]. Filled and empty circles indicate transition energies obtained with a (12,12) and (14,14) active spaces, respectively.

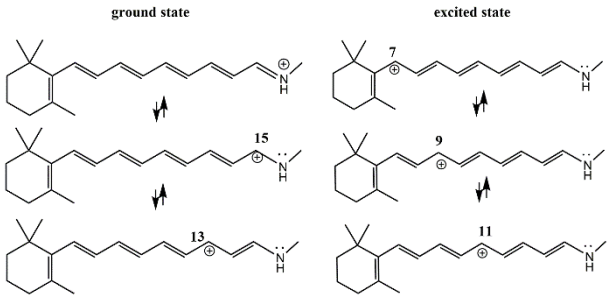

Scheme 2. The most important mesomeric structures in ground and excited state of rPSBs.

2. Influence of the Functionalization on the Character of the Bright Excited State

In the previous section, we demonstrated that through modification of the rPSB backbone with functional groups it becomes possible to fine-tune the absorption energy over the whole visible range in a similar way to what can be achieved by applying a homogenous external EF. In this section, we go one step further and investigate the effect that the functionalization has on the topology of the S_1 state in the Franck-Condon (FC) region. As established previously for R[7], blue- and red-shifts of the energy of S_1 (CT state) by a moderate (i.e. ±0.003 au) external EF lead to the energetic proximity and wavefunction mixing with either S_2 (for positive fields) or S_0 (for negative fields), both of covalent nature and, hence, less affected by the functionalization.

The wavefunction mixing is reflected in the bond order of the conjugated chain at the S_1 equilibrium geometry. Specifically, bond relaxation in the presence of moderate fields does not invoke the single-double bond inversion documented in the absence of an EF but rather leads to bond length equilibration[7]. Following the analogy between the application of an external field and the chemical functionalization of rPSB, we find a correlation between the bond order of the relaxed S_1 geometry and the functionalization pattern. In the following, we use the sensitivity of bond lengths to the nature of the excited state to categorize the functionalized systems in five different groups (**Figure 2**). As a quantifying criterium we employ the bond length alternation (BLA, for exact definition see caption of **Figure 2**) at the relaxed excited state geometry and correlate it to the absorption energy which is itself correlated to the strength of the interaction between the conjugated chain and the substituents:

i- Reference (normal BLA) region: comprises a number of mostly mono-functionalized systems (R_{20}-R_{32}). This group exhibits a clear N-head to C-tail CT in the lowest ES and a large S_1-S_0 and S_1-S_2 gaps. Consequently, ES relaxation reaches a minimum characterized with the “classical” inverted single-double bond order established for R (BLA > 0.035). The same behavior has been shown for the R under the effect of an external EF of -0.0025 to +0.0020 au. Consequently, systems in this region are expected to exhibit an EF profile like that of the bare rPSB, i.e. triggering ultrafast decay and photoisomerization.

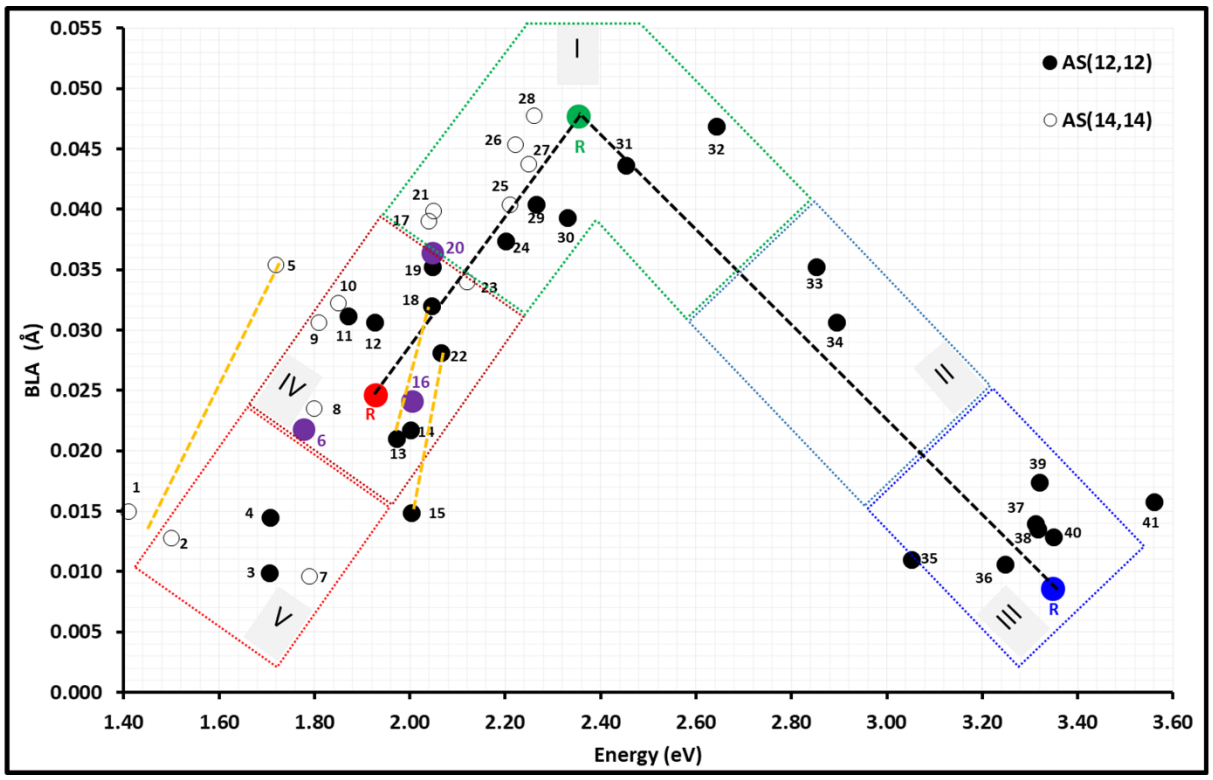

Figure 2. Correlation between the absorption energy and BLA of the relaxed geometries. Bond length alternation (***BLA***) parameter defined as $\boldsymbol{BLA} = \sum_{i=7}^{14}|\boldsymbol{d}_{c_i-c_{i+1}} - \mathbf{1.41}|/\mathbf{8}$, with $\boldsymbol{d}_{c_i-c_{i+1}}$ the bond length between carbon atoms i and i+1 from the conjugated chain. In the planar, fully conjugated chains R_6, R_{11}, R_{20}, R_{21}, R_{24} and R_{29} the ***BLA*** was calculated over the whole conjugated chain. Labelling according to **Scheme 1**. Black dashed lines show the behaviour of R in the presence of a uniform external EF (±0.003au.)[7]. Yellow dashed lines indicate sub-groups of compounds which show deviations from the global trend. Filled and empty circles indicate transition energies obtained with a (12,12) and (14,14) active spaces, respectively.

ii- Weakly blue-shifted (intermediate BLA) region: comprises systems absorbing in the blue with respect to R in the spectral region 2.70-3.10 eV [1] (R_{33} and R_{34}) characterized by an S_1 wavefunction which shows partial CT/covalent mixing (still dominated by the CT configuration) due to the progressively decreasing energy gap between S_1 and the covalent S_2, causing a less pronounced BLA (0.020 < BLA < 0.035). This is equivalent to the effect observed for R for intermediate EF strengths of +0.0020 to +0.0025.

iii- Strongly blue-shifted (nearly equilibrated BLA) S_1/S_2 mixing region: comprises mostly doubly functionalized systems (R_{35}−R_{41}) with absorption energies above 3.10 eV. This corresponds to the effect achieved by applying an EF > +0.0025 au to R. In those systems, the wavefunctions of the nearly isoenergetic S_1 and S_2 states are mixing strongly so that almost no single-double bond length inversion is observed upon relaxation (0.005 < BLA < 0.020). Such strong shifts are only feasible by introducing a positively charge group close to the C-terminus (R_{39}, R_{41}) or by utilizing the synergic effect of suitably positioned pairs of functional groups. To that aim, we introduced a CF_3 group close to the ß-ionone ring and groups with ***M*** effect (-OR and -NR_2) close to the N-terminus.

iv- Weakly red-shifted (intermediate BLA) region: comprises systems absorbing in the red with respect to R in the spectral region 1.80-2.10 eV (R_{10}-R_{14}, R_{16}-R_{19}) characterized by an S_1 wavefunction which shows partial CT/covalent mixing with the covalent GS (still dominated by the CT configuration) causing a less pronounced BLA (0.020 < BLA < 0.035). This is equivalent to the effect observed for R under intermediate EF of -0.0030 to -0.0025 au.

v- Strongly red-shifted (nearly equilibrated BLA) S_0/S_1 mixing region: comprises mostly doubly functionalized systems (R_1-R_4, R_6, R_7) with absorption energies below 1.80 eV. This corresponds to the effect achieved by applying an EF < -0.0030 au to R. In those systems we observe an inversion of the ionic/covalent character of S_0 and S_1, so that almost no single-double bond length inversion is observed upon relaxation (0.005 < BLA < 0.020). As elucidated previously, strong shifts are only feasible by introducing an electron rich heteroaromatic ring (R_1, R_2) and/or by

[1] *The specified spectral window should be understood as a guide to the eye, as compounds absorbing at the same wavelength could exhibit BLA parameters that would put them in adjacent regions depending on the strength of the interaction between the conjugated chain and the functional group.*

utilizing the synergic effect of suitably positioned pairs of functional groups (R_2, R_3, R_4, R_7). To that aim, we introduced a CF_3 group close to the N-head and groups with ***M*** effect (-O- and -NR-) close to the C-terminus.

As shown in **Figure 2**, most of the systems follow the trend established for R in the presence of a homogeneous external EF (dashed black lines in **Figure 2**) and can be classified based on the correlation between BLA and the absorption energy. However, in the course of the study we encountered few outliers to the expected behavior (R_1, R_5, R_{15}, R_{41}). Taking a closer look at the dataset, we identified sub-groups of functionalized rPSB which exhibit distinctive trends (yellow dashed lines in **Figure 2**) reflecting the overall trend. The sub-groups [R_{22}, R_{14}, R_{15}] and [R_{13}, R_{16}, R_{18}] involve -NR_2 and -OR substituents at C_9, respectively. The absorption energy of these compounds is less affected by the the substituent, in stark contrast with the excited BLA. The resulting steeper trend line with respect to the overall trend indicates that the hetero-groups are weakly conjugated to the chain in the GS whereas in the ES the degree of conjugation depends on their composition. The sub-group [R_1, R_2, R_5] which contains the outliers R_1 and R_5 exhibits a hetero-aromatic ring functionalized at the C-tail of the rPSB as a common feature. This sub-group is characterized with a trend line red-shifted by ca. 0.2 eV with respect to the overall trend, which can be interpreted considering the strong conjugation to the main chain in the GS.

3. Influence of the Functionalization on the Excited State trans-cis Isomerization Path

To complete the study, we demonstrate how the functionalization affects the topology of the PES of the bright ES along the photoinduced trans-cis isomerization.

It is well known that in R in absence of external EF the isomerization occurs in an ultrafast fashion (within 100 fs inside the protein cavity) mediated by a CI seam intersecting the essentially barrierless minimum energy path around 90° torsion[4, 8, 13]. In our previous study on the effects of external EF on the isomerization of R, we observed for weak positive EF a steeper S_1 path towards the CI region, implying a speed-up of the isomerization[8]. In a recent comparative study of three visual pigments Rhodopsin, Squidrhodopsin and Melanopsin, containing the same rPSB chromophore whose absorption energy is electrostatically modulated inside the protein cavity in a way mimicking effects by external weak positive fields, we confirmed this observation by demonstrating a correlation between absorption energy and lifetime[4].

Applying a negative EF, we observed[8] a progressive covalent/ionic wavefunction mixing in the FC region which leads to the gradual inversion of the ES character along the torsional path towards the S_0/S_1 conical intersection. For moderate negative fields the covalent configuration may become dominant already at the relaxed planar excited state geometry and this may alter completely the profile of the EF PES towards the CI. An in-depth analysis of R reveals that bond length equilibration in the relaxed S_1 state is achieved in gas-phase for values of the EF strength between -0.0025 and -0.0030 au with an optimal value at -0.0027 au for which the BLA is 0.016. Such an EF red-shifts the absorption energy of R to 1.95 eV with respect to the field-free case (2.36 eV).

The categorization performed in the previous section (**Figure 2**) puts functionalized rPSB chromophores with absorption energies around 1.95 eV in the weakly red-shifted region IV with BLA values of the relaxed ES geometries around 0.020-0.035. This region is particularly intriguing as it lies between the normal and the equilibrated BLA regions. Thus, by applying positive and negative external EFs in the order of few MV/cm to compounds belonging to this window we anticipate to be able to shift their absorption energy in the neighboring BLA regions I and V, respectively, where, based on the gathered knowledge regarding the potential energy profiles of R for different EF strengths[7], we expect to observe a markedly different behavior. In particular, we expect a barrierless ES minimum energy path from the FC point to the CI region when the system's absorption energy is blue-shifted in the reference region I, whereas we expect a sloped path towards an energetically higher lying CI when the system's absorption energy is red-shifted to the strongly red-shifted region V. Hence, within the approximations of the current theoretical set up, functionalized rPSB from the weakly red-shifted region bare the potential for selective switch on/off their ultrafast isomerization behavior by applying external EFs of low intensity.

In order to test this idea, we selected compound R_{16}, see Scheme 1. R_{16} displays an ordinary single-double bond alternation, absorbs at 2.01 eV and exhibits a modest BLA of 0.024, thus it belongs to group IV. Applying a moderate EF of +0.001 au and -0.001 au, shifts its absorption energy to 2.09 eV and 1.94 eV and its BLA to 0.036 and 0.009, respectively, thus placing the system exposed to the external EF in regions I and V. We performed relaxed ES scans along several torsional coordinates:

- +0.001 au: bonds C_9-C_{10}, C_{11}-C_{12} and C_{13}-C_{14} (**Figure 3**, left column) which display a clear single bond character at the relaxed ES geometry due to the “classical” single-double bond alternation with respect to the GS equilibrium.

- -0.001 au: bonds C_8-C_9, C_9-C_{10}, C_{10}-C_{11}, C_{11}-C_{12}, C_{12}-C_{13} and C_{13}-C_{14} (**Figure 3**, right column and **Figure S1** in SI) as the relaxed ES geometry displays bond equilibration rather than bond alternation.

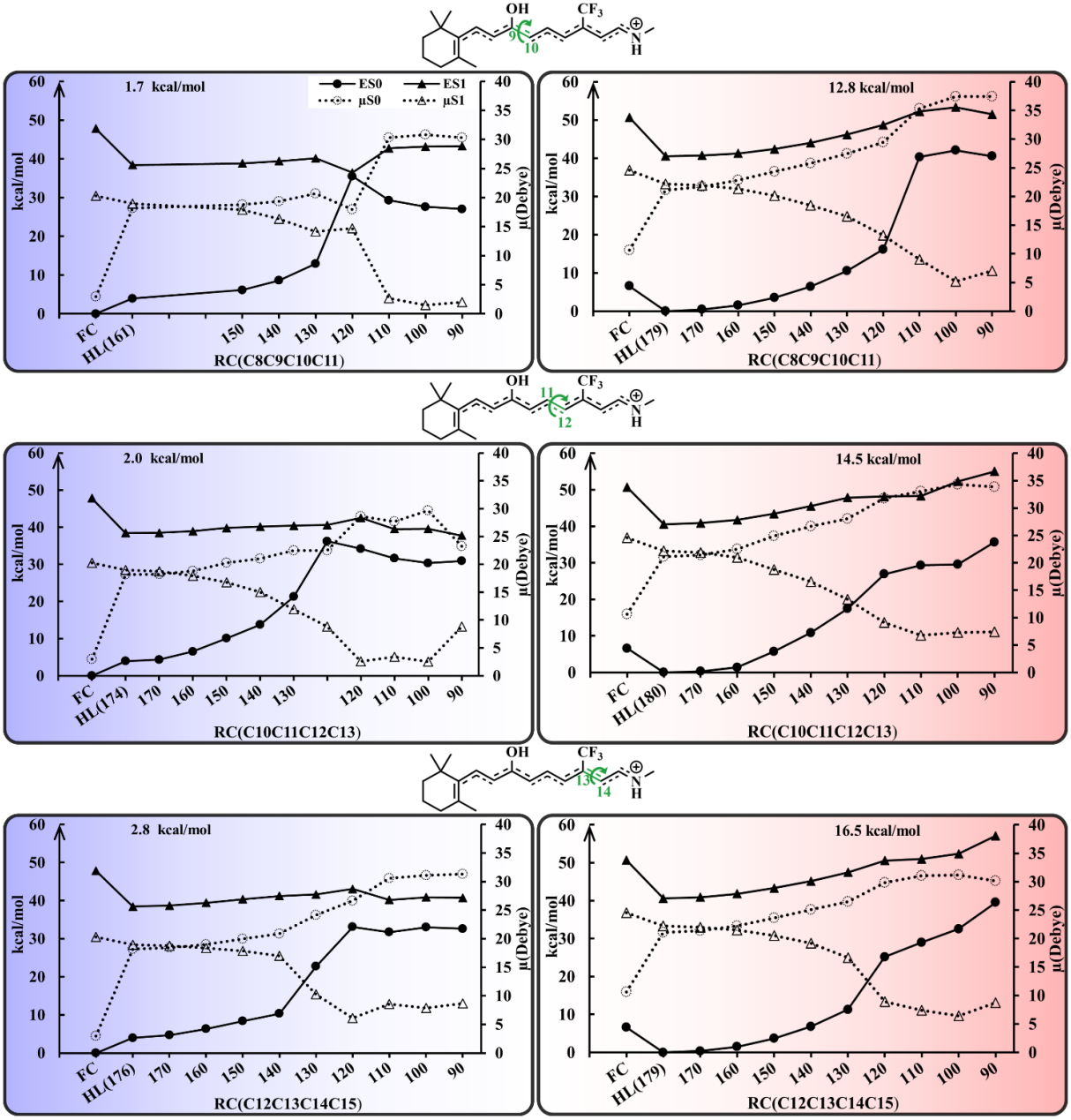

Figure 3. Energy profiles (solid lines) and dipole moment values (dashed lines) of R_{16} (belongs to group IV, see **Figure 2**) along three torsion angles (C_9–C_{10}, C_{11}–C_{12}, and C_{13}–C_{14}) obtained from ES relaxed scans in the presence of an EF of +0.001 au (left column) and -0.001 au (right column). The energy height of the barrier is reported on the top of the panel for each profile. "HL" denotes the S_1 planar minimum.

Figure 3 displays the profiles around the bonds C_9-C_{10}, C_{11}-C_{12} and C_{13}-C_{14} in both positive and negative EF (see SI for profiles along the remaining bonds). In contrast to R which has a barrierless excited state profile, R_{16} exhibits a finite barrier which connects a (nearly) planar minimum (denoted **HL** in **Figure 3**) with the (avoided) crossing region. For positive EFs (**Figure 3**, left column) we obtain small energy barriers around ca. 2-3 kcal/mol. Thereby, the height of the barrier is directly correlated to the distance from the N-head. Moreover, we observe a pre-twisting of the relevant bond upon ES relaxation up to 20° as in the case with C_9-C_{10}. For negative EFs (**Figure 3** right column) the energy profiles for torsion around the same bonds exhibit an order of magnitude larger barriers and do not access a real crossing with the GS. Instead, we encounter comparable barriers of ca. 2 kcal/mol along C_{10}-C_{11} and C_{12}-C_{13} (see **Figure S1** in the SI) leading to a real crossing. Notably, the crossing with the GS occurs at highly twisted geometries at 90°-100°.

The example of R_{16} corroborates the idea that moderate ESs applied to suitably functionalized rPSB facilitate their shift between neighboring BLA regions associated with a significant change of the PES profile. The example also shows the subtle

interplay between the covalent and ionic character which favors isomerization around different bonds in the different BLA regions.

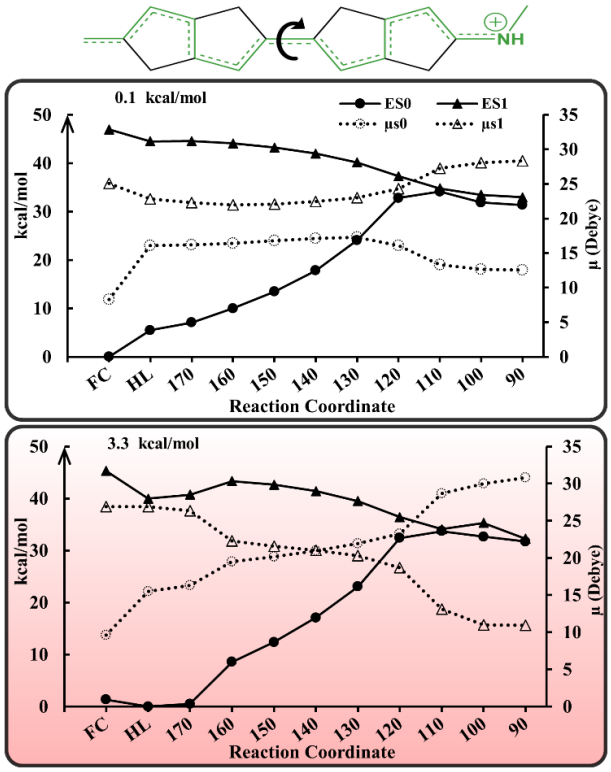

Figure 4. Energy profiles along excited state relaxed scans around bond C_9−C_{10} of R_{20} (located at the border between regions IV and I, **Figure 2**) calculated in the absence (top) and in the presence of an external EF of -0.001 au (bottom). The energy height of the barrier is reported on the top of the panel for each profile. "HL" denotes the S_1 planar minimum.

4. *In silico* design of rPSB: switching on/off of the ultrafast isomerization behavior through field modulation

Capitalizing on the gathered insights regarding the synergic effects of functionalization and external EFs we are in the position to formulate a protocol for controlling the photophysical behavior of rPSB, thereby turning it from an ultrafast non-radiative isomerizing device into a fluorescent dye in three synthetic steps:

a) introduce suitably placed functional groups that would shift the absorption spectrum of the chromophore in the red spectral window (600-650 nm)

b) block torsion around bonds in the vicinity of the N-head, e.g. by constraining them in rings

c) control the isomerization behavior by applying an external EF with a moderate strength (±0.001 au) as compared to the one needed to reach the same effects for R

This protocol is illustrated based on compound R_{20}. R_{20} is a planar all-*trans* rPSB with seven double bonds constrained in two ring formations. With an absorption energy of 2.05 eV R_{20} is located rather at the border between *reference* and *weakly red-shifted* regions (**Figure 2**), displaying, correspondingly, a rather large BLA of 0.035. Nevertheless, R_{20} is particularly tempting for control purposes as it offers a single free double bond (C_9-C_{10}) for photoisomerization. **Figure 4** shows a relaxed scan around the free bond in the absence and presence of an external EF. As for all members of the *reference region* I a barrierless excited state profile is encountered in the absence of an external EF which drives the system towards a CI around 120°. This agrees with the bond inversion of the central bond to 1.47 Å in the relaxed S_1 geometry. Application of a homogeneous external EF of just -0.001 au, which red-shifts the absorption energy by ca. 0.1 eV to 1.92 eV, lowers dramatically the BLA to 0.017. Notably, the central bond elongates to just 1.40 Å at the relaxed S_1 geometry which is found to be a local minimum connected with a barrier of 3.3 kcal/mol to the CI region.

Although the above example is a neat proof of the concept, we recognize that R_{20} can be improved further. Specifically, we want to make use of the possibility to apply an electric field in both directions, thereby increasing the modulation range as shown in the previous section for R_{16}. It is evident that application of a positive EF to R_{20} is of no avail as already in the absence of an EF there is virtually no ES barrier to surmount, (**Figure 4**, top). It would be desirable to have a finite barrier along S_1 in the absence of EF that could be: a) suppressed through a positive field; b) increased through a negative EF. To achieve this goal, we modified R_{20} with a -OMe group at C_5, the only available position for functionalization in the vicinity of the C-terminus, thus obtaining compound R_6. As expected, the functionalization with this *+M* group enforces a 0.25 eV red-shift of the absorption energy accompanied by a near equilibration of all bond lengths upon S_1 relaxation (C_9-C_{10} acquiring a value of 1.41 Å), thus placing the system at the border between the *weakly* and *strongly red-shifted regions* (**Figure 2**). **Figure 5** shows the excited state profiles of R_6 in the absence of EF (middle), as well as for moderate positive (top) and negative (bottom) EFs of ±0.001 au. In contrast to R_{20}, in the absence of an external EF R_6 exhibits a finite barrier along the torsional coordinate of 2.2 kcal/mol peaking around 150°, suggesting a slowed down isomerization with respect to R. In the presence of a positive EF the barrier decreases to 1.0 kcal/mol, thereby shifting the transition state towards the FC region to 160° (**Figure 5**, top). On the other hand, in the presence of a negative EF S_1 acquires a flat profile with no pronounced gradient towards what is now an avoided crossing region (**Figure 5**, bottom).

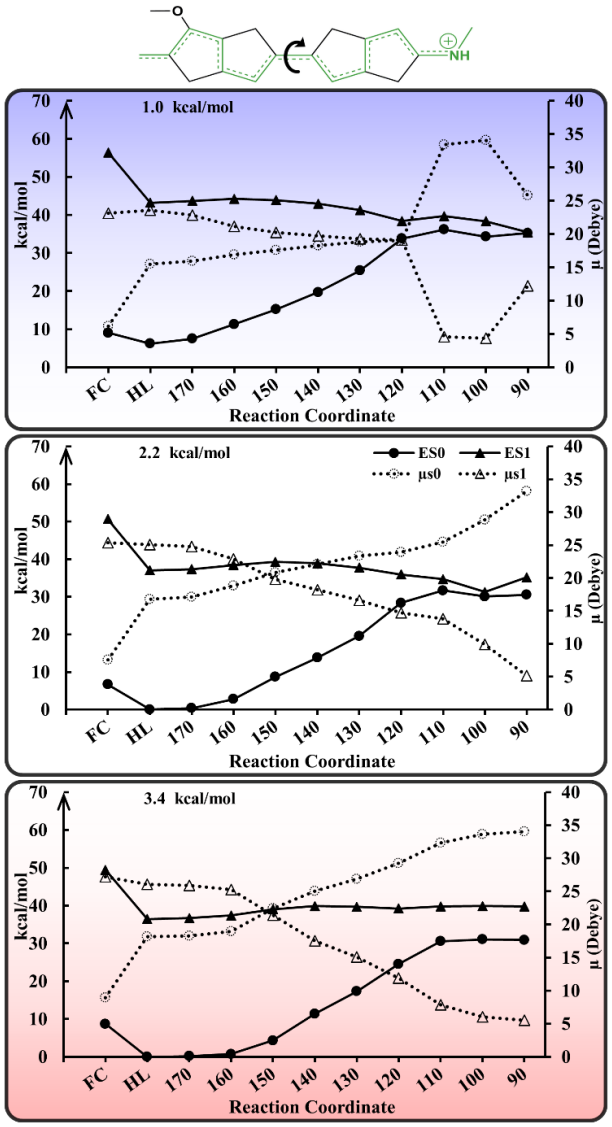

Figure 5. Energy profiles along ES relaxed scans around bond C_9–C_{10} of R_6 (located at the border between regions V and IV, **Figure 2**) calculated in the absence (middle) and in the presence of an external EF of +0.001 au (top) and -0.001 au (bottom). The energy height of the barrier is reported on the top of the panel for each profile. "HL" denotes the S_1 planar minimum.

Conclusion

Understanding, regulating and tuning spectral and photochemical properties is currently one of the most important goals targeted in the designing of new optoelectronic molecular devices. rPSBs undergo ultrafast *cis-tans* isomerization around specific double bonds, which makes them important candidate for designing efficient photo-reversible molecular switches. In our pervious study we proved that the absorption of rPSB can be gently regulated under the effect of external homogenous EFs[8]. Here, we provide an alternative way to fine-tune its absorption over the entire visible spectrum. This way is based on the modification of the retinal backbone with functional groups acting as generators of local EFs that are eventually able to mimic the effects previously observed for external homogenous EFs.

Beyond this, the functionalization affects not only the absorption energy but also the topology of the PES of the bright ES that drives the photoinduced *trans-cis* isomerization path. Specifically, we demonstrated that for a variety of compounds there is a correlation between the absorption energy and the S_1 geometry of the ES. We exploited this correlation to rank the functionalized systems into five different classes according to their BLA and vertical excitation energies. We observe that, by applying much weaker (compared to the ones needed for R) positive and negative external EFs on compounds from class IV (**Figure 2**), photo-reactivity is altered to resemble compounds from the neighboring BLA regions I (normal BLA, quasi-barrierless profile towards the CI) and V (nearly equilibrated BLA, steep barrier towards the CI), respectively. We exploited this behavior to demonstrate for a representative compound of class IV (R_{16}) how the photoisomerization propensity can be enhanced or decreased in practice under the effect of external EFs in the few MV/cm range. Eventually, the synergic effects of functionalization and external EFs have been applied to achieve a regioselective photoisomerization that can be reversibly switched on/off (and, in turn, emission can be reversibly switched off/on). This marks a promising step toward the design of bio-inspired reversibly switchable fluorescent/non-fluorescent non-photoisomerizing/ photoisomerizing molecular devices.

Acknowledgements

Financial support from the PHANTOMS project, PRIN: PROGETTI DI RICERCA DI RILEVANTE INTERESSE NAZIONALE–Bando 2017, Prot. 2017A4XRCA, is acknowledged.

Keywords: photoisomerization control• electric field• potential energy surface• functional group• CASPT2

References

[1] aK. Palczewski, *J. Biol. Chem.* **2012**, *287*, 1612-1619; bJ. L. Spudich, C. S. Yang, K. H. Jung, E. N. Spudich, *Annu. Rev. Cell Dev. Biol.* **2000**, *16*, 365-392; cR. A. Bogomolni, J. L. Spudich, *Biophys. J.* **1987**, *52*, 1071-1075; dS. Yokoyama, T. Tada, H. Zhang, L. Britt, *Proc. Natl. Acad. Sci. U. S. A.* **2008**, *105*, 13480-13485.

[2] aA. K. Sharma, J. L. Spudich, W. F. Doolittle, *Trends Microbiol.* **2006**, *14*, 463-469; bK. Nakanishi, *Am. Zool.* **1991**, *31*, 479-489; cR. A. Mathies, C. H. Brito Cruz, W. T. Pollard, C. V. Shank, *Science* **1988**, *240*, 777-779; dJ. Herbst, K. Heyne, R. Diller, *Science* **2002**, *297*, 822-825; eT. Kobayashi, T. Saito, H. Ohtani, *Nature* **2001**, *414*, 531-534; fA. Yabushita, T. Kobayashi, *Biophys. J.* **2009**, *96*, 1447-1461; gJ. E. Kim, M. J. Tauber, R. A. Mathies, *Biochemistry* **2001**, *40*, 13774-13778.

[3] aG. Bassolino, T. Sovdat, M. Liebel, C. Schnedermann, B. Odell, T. D. Claridge, P. Kukura, S. P. Fletcher, *J. Am. Chem. Soc.* **2014**, *136*, 2650-2658; bS. Rinaldi, F. Melaccio, S. Gozem, F. Fanelli, M. Olivucci, *Proc. Natl. Acad. Sci. U. S. A.* **2014**, *111*, 1714-1719; cS. Gozem, H. L. Luk, I. Schapiro, M. Olivucci, *Chem. Rev.* **2017**, *117*, 13502-13565; dJ. P. Malhado, J. T. Hynes, *J. Chem. Phys.* **2016**, *145*, 194104; eT. Kobayashi, A. Yabushita, *J. Lumin.* **2008**, *128*, 1038-1042; fP. Coto, A. Sinicropi, L. De Vico, N. Ferre, M. Olivucci, *Mol. Phys.* **2006**, *104*, 983-991.

[4] M. M. El-Tahawy, A. Nenov, O. Weingart, M. Olivucci, M. Garavelli, *J Phys Chem Lett* **2018**, *9*, 3315-3322.

[5] aR. S. Liu, G. S. Hammond, *Photochem Photobiol Sci* **2003**, *2*, 835-844; bF. DeLange, P. H. Bovee-Geurts, J. VanOostrum, M. D. Portier, P. J. Verdegem, J. Lugtenburg, W. J. DeGrip, *Biochemistry* **1998**, *37*, 1411-1420; cF. Derguini, K. Nakanishi, *Photobioch Photobiop* **1986**, *13*, 259-283; dE. Kloppmann, T. Becker, G. M. Ullmann, *Proteins: Structure, Function, and Bioinformatics* **2005**, *61*, 953-965; eV. R. Kaila, R. Send, D. Sundholm, *J. Phys. Chem. B* **2012**, *116*, 2249-2258; fK. Shimono, Y. Ikeura, Y. Sudo, M. Iwamoto, N. Kamo, *Biochim. Biophys. Acta* **2001**, *1515*, 92-100; gM. Ruckenbauer, M. Barbatti, T. Muller, H. Lischka, *J. Phys. Chem. A* **2013**, *117*, 2790-2799; hE. C. Yan, M. A. Kazmi, Z. Ganim, J. M. Hou, D. Pan, B. S. Chang, T. P. Sakmar, R. A. Mathies, *Proc. Natl. Acad. Sci. U. S. A.* **2003**, *100*, 9262-9267.

[6] aS. Y. Kim, S. A. Waschuk, L. S. Brown, K. H. Jung, *Biochim. Biophys. Acta* **2008**, *1777*, 504-513; bR. M. Crist, C. Vasileiou, M. Rabago-Smith, J. H. Geiger, B. Borhan, *J. Am. Chem. Soc.* **2006**, *128*, 4522-4523; cC. Vasileiou, S. Vaezeslami, R. M. Crist, M. Rabago-Smith, J. H. Geiger, B. Borhan, *J. Am. Chem. Soc.* **2007**, *129*, 6140-6148; dM. M. Huntress, S. Gozem, K. R. Malley, A. E. Jailaubekov, C. Vasileiou, M. Vengris, J. H. Geiger, B. Borhan, I. Schapiro, D. S. Larsen, M. Olivucci, *J. Phys. Chem. B* **2013**, *117*, 10053-10070; eW. Wang, Z. Nossoni, T. Berbasova, C. T. Watson, I. Yapici, K. S. Lee, C. Vasileiou, J. H. Geiger, B. Borhan, *Science* **2012**, *338*, 1340-1343; fW. Wang, J. H. Geiger, B. Borhan, *Bioessays* **2014**, *36*, 65-74; gC. Vasileiou, W. Wang, X. Jia, K. S. Lee, C. T. Watson, J. H. Geiger, B. Borhan, *Proteins* **2009**, *77*, 812-822; hD. Man, W. Wang, G. Sabehi, L. Aravind, A. F. Post, R. Massana, E. N. Spudich, J. L. Spudich, O. Beja, *EMBO J.* **2003**, *22*, 1725-1731; iS. Ganapathy, O. Becheau, H. Venselaar, S. Frolich, J. B. van der Steen, Q. Chen, S. Radwan, J. Lugtenburg, K. J. Hellingwerf, H. J. de Groot, W. J. de Grip, *Biochem. J* **2015**, *467*, 333-343.

[7] aB. Honig, A. Nicholls, *Science* **1995**, *268*, 1144-1149; bI. T. Suydam, C. D. Snow, V. S. Pande, S. G. Boxer, *Science* **2006**, *313*, 200-204; cI. T. Suydam, S. G. Boxer, *Biochemistry* **2003**, *42*, 12050-12055.

[8] M. M. El-Tahawy, A. Nenov, M. Garavelli, *J. Chem. Theory Comput.* **2016**, *12*, 4460-4475.

[9] M. Alemani, M. V. Peters, S. Hecht, K.-H. Rieder, F. Moresco, L. J. J. o. t. A. C. S. Grill, **2006**, *128*, 14446-14447.

[10] aM. Manathunga, X. Yang, M. Olivucci, *J Phys Chem Lett* **2018**, *9*, 6350-6355; bQ. Wang, G. G. Kochendoerfer, R. W. Schoenlein, P. J. Verdegem, J. Lugtenburg, R. A. Mathies, C. V. Shank, *J Phys Chem* **1996**, *100*, 17388-17394; cD. Koch, W. Gärtner, *Photochem. Photobiol.* **1997**, *65*, 181-186; dP. Verdegem, P. Bovee-Geurts, W. De Grip, J. Lugtenburg, H. De Groot, *Biochemistry* **1999**, *38*, 11316-11324; eR. S. Becker, K. Freedman, *J. Am. Chem. Soc.* **1985**, *107*, 1477-1485; fM. A. Verhoeven, P. H. Bovee-Geurts, H. J. de Groot, J. Lugtenburg, W. J. DeGrip, *J. Mol. Biol.* **2006**, *363*, 98-113; gI. Schapiro, *J. Phys. Chem. A* **2016**, *120*, 3353-3365; hH. Kandori, H. Sasabe, K. Nakanishi, T. Yoshizawa, T. Mizukami, Y. Shichida, *J. Am. Chem. Soc.* **1996**, *118*, 1002-1005; iT. Sovdat, G. Bassolino, M. Liebel, C. Schnedermann, S. P. Fletcher, P. Kukura, *J. Am. Chem. Soc.* **2012**, *134*, 8318-8320; jK. Nakanishi, R. Crouch, *Isr. J. Chem.* **1995**, *35*, 253-272; kW. Gaertner, D. Oesterhelt, *Eur. J. Biochem.* **1988**, *176*, 641-648.

[11] B. Demoulin, S. F. Altavilla, I. Rivalta, M. Garavelli, *J Phys Chem Lett* **2017**, *8*, 4407-4412.

[12] I. Conti, F. Bernardi, G. Orlandi, M. Garavelli, *Mol. Phys.* **2006**, *104*, 915-924.

[13] D. Polli, P. Altoe, O. Weingart, K. M. Spillane, C. Manzoni, D. Brida, G. Tomasello, G. Orlandi, P. Kukura, R. A. Mathies, M. Garavelli, G. Cerullo, *Nature* **2010**, *467*, 440-443.

Entry for the Table of Contents (Please choose one layout)

Layout 1:

RESEARCH ARTICLE

Text for Table of Contents

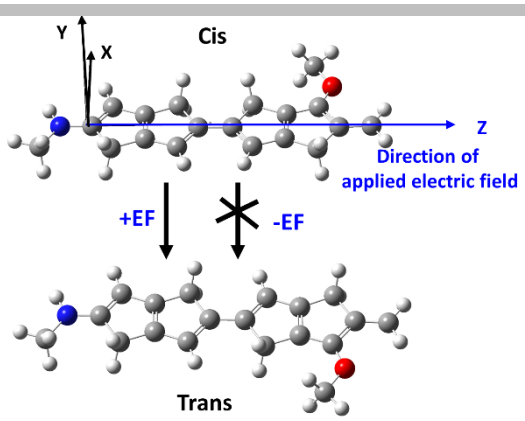

Author(s), Corresponding Author(s)*

Page No. – Page No.

Title